Predictive Modelling Study of Prosthetic-Socket Temperature Evolution

Ugochi Chinomso Uregbulam[*1,2], Olabode Thomas Olakoyejo[2], Manasseh Babale Shitta[4], Adebayo Adeyemi Ogundare[2], Gamaliel Adetoluwafe Adebayo[1,3], Chiemezie Precious Jacob[1], Ibrahim Ademola Fetuga[5], Joseph Ifeolu Orisaleye[6,7], Adekunle Omolade Adelaja[2]

[1]Department of Biomedical Engineering, University of Lagos, Akoka-Yaba, Lagos 101017 Nigeria
[2]Department of Mechanical Engineering, University of Lagos, Akoka-Yaba, Lagos 101017 Nigeria
[3]Medical Artificial Intelligence Laboratory (MAI Lab), Lagos, Nigeria
[4]National Centre for Energy Efficiency and Conservation, University of Lagos, Nigeria
[5]Clarkson University, NY, USA
[6]Birmingham City University, United Kingdom
[7]Durban University of Technology, Durban, South Africa
[*]Corresponding Author Email curegbulam@unilag.edu.ng, ORCID: 0009-0000-7486-4272

Abstract
Liner material selection plays a critical role in the overall well-being and quality of life of lower-limb prosthesis users. More than half of lower-limb prosthesis users report thermal-related issues due to prosthetic liner materials necessitating the optimisation of material selection for improved heat dissipation. Recent research efforts to improve heat dissipation and moisture mitigation indicate that liner design and material optimization remain crucial in the heat dissipation process within the prosthesis. In this study, a data-driven, predictive modelling approach is proposed to evaluate and optimize liner material selection and aid thermal discomfort solution efforts. A 3600-point prosthetic socket temperature dataset was collected under realistic ambient conditions using ANSYS CFD simulations. These data were then processed through a modelling pipeline comprising data preprocessing and autoregressive integrated moving average (ARIMA) Forecasting. The ARIMA model forecast, using the 3600-point data, showed an appropriate initial heating phase followed by stabilization at approximately 30 ℃. This demonstrates a plausible long-term temperature trajectory, which is crucial for material selection and thermal comfort optimization in prosthetic applications.

Keywords: ARIMA forecasting, data augmentation, heat dissipation, predictive modelling, prosthesis

Nomenclature

c_b	specific heat capacity of blood, J/(kg K)
c_t	specific heat capacity of tissue, J/(kg K)
k_t	tissue heat conductivity, W/(m K)
$q_{m,bas}$	basal heat generation caused by cell metabolism, W/m^3
T_b	blood temperature, K
T_t	tissue temperature, K
∇	gradient operator, dimensionless

Greek Symbols

ρ_t	tissue density, kg/m^3
ρ_b	blood density, kg/m^3

`

ω_b blood perforation rate or volumetric rate of perfusion, mL/(mL s)

1.0 INTRODUCTION

Thermal discomfort is a major concern for lower-limb prosthesis users. Studies report that roughly half of amputees experience significant heat or sweating issues in the socket (Edwards et al., 2025). Conventional socket and liner materials tend to trap heat, disrupting the body's normal thermoregulation. Consequently, amputees often report excessive perspiration, skin irritation, and reduced prosthesis use due to heat-related discomfort (Edwards *et al*., 2025). These effects not only diminish user comfort but can also threaten tissue health and functional outcomes of the treatment. A lower limb prosthesis is an artificial device that replaces a missing part of the human body (Williams, 2020). They are vital devices for amputees, as their primary function is to return patients to their state of life before amputation. It enables amputees to perform their daily activities as a physically able person (Nurhanisah *et al*., 2019).

The relationship between the measured skin temperature and perceived discomfort is complex. Diment et al. (2019) found that both the residual and contralateral limbs cooled during exercise, and that changes in the residual-limb skin temperature did not predict the wearer's thermal discomfort (Mathur et al., 2016). According another research, skin temperature does not explain the thermal discomfort experienced (Paternò *et al*., 2020), implying that subjective heat sensation involves more than just heat accumulation.

Amputation reduces the total body surface area (BSA) by approximately 9% for transtibial amputation (below-knee) and 21% for transfemoral amputation (Williams, 2020), thereby disrupting thermoregulation within the body (Ghoseiri and Safari, 2014). All heat transfer mechanisms including conduction, convection and radiation are disturbed due to the reduced BSA and the insulative prosthetic barrier possessing low thermal conductivity. The prosthetic material creates a closed environment that prevents ventilation and air circulation between the prosthesis and the environment thereby causing heat to be trapped inside the socket (Williams, 2020).

During physical activity, metabolic heat production increases from the resting state. This increased metabolic rate results in a high body temperature, specifically, in the lower limbs. The body is homeothermic, generally maintaining a core temperature of approximately 36.8±1°C, but the body temperature rises with physical activity (Nurhanisah *et al*., 2019). For example, a 10-minute treadmill walk can increase the limb temperature by about 0.8°C, and a 30-minute walk can increase it about 3.1°C (Abbood *et al*., 2017).

Recent research has explored advanced liner technologies such as phase-change material (PCM) or integrated cooling channel for improving thermal regulation. For example, phase-change-material (PCM) liners and vented sockets have been developed to better control the microclimate in the socket (Fiedler *et al*., 2022; Gnyawali *et al*., 2023). Early trials have shown promise but also limitations. A randomized crossover trial comparing PCM liners to conventional liners found that PCM liners tended to slow the rise in limb temperature and improve prosthesis use, but these effects did not reach statistical significance (Fiedler et al., 2022). Similarly, a recent study of vented socket systems (Gnyawali *et al*., 2023) demonstrated significant reductions in interface humidity with a vented liner, but no notable change in skin temperature. These results suggest that although novel liner designs can alter short-term heat transfer, there is a need to investigate long-term thermal build-up. Therefore, a deeper and more predictive understanding of socket thermodynamics is needed to create more efficient solutions (Gnyawali *et al*., 2023).

To fill this gap, this study proposes a data-driven, predictive modelling approach to evaluate and optimize liner materials (Lee *et al*., 2023). Machine learning and time-series models can capture the complex heat transfer dynamics at the limb-liner interface. For instance, Mathur *et al*. (2016)

`

developed a Gaussian Process model that uses the thermal time constants of socket materials to predict residual limb skin temperature from in-socket measurements. Likewise, classical forecasting tools such as the autoregressive integrated moving average (ARIMA) model, are well established for extending short-term data into longer forecasts. ARIMA models are widely used in clinical and engineering time-series analysis, especially for health data and temperature-related environment indices where autocorrelation and trend are present. ARIMA is a useful tool for use to handle autocorrelation in clinical data (Schaffer *et al*., 2021), hybrid modelling including ARIMA has been known to result in a better ability to capture patterns of time series involving environment and health leading to improved environmental/thermal forecasting (Kaur *et al*., 2023).

Across health, environmental and engineering time-series forecasting, ARIMA is generally known to be effective for short to medium term forecasting of univariate, approximately linear, stationary signals, including temperature related series (Kaur *et al*., 2023). As a baseline, ARIMA is useful for benchmarking and for cases with limited data or where model simplicity is preferred (Feng *et al*., 2022).

Alternative approaches in prosthetics, skin temperature and related biomedical time series work include the Gaussian Processes (GP) where researchers used it to predict residual limb skin temperature in lower limb prostheses (Mathur *et al*., 2016). Another alternative approach is the Long Short Term Memory Network (LSTM) which is used for physiological and environmental time-series forecasting (Feng *et al*., 2022).

ARIMA was selected for the present analysis because the skin temperature series exhibited strong thermal dependence and approximate linearity, and because ARIMA offers interpretability, modest data requirements, and a well understood statistical framework suitable for clinical and engineering applications (Schaffer *et al*., 2021; Patharkar *et al*., 2024).

2.0 METHODOLOGY

2.1 *Geometry Description*

A lower limb prosthesis consists of prosthetic elements like the socket, pylon and prosthetic foot. The socket houses the residual limb (**Figure 1a**). A computer aided design (CAD) model of the residual limb and prosthesis was produced and imported into ANSYS CFD. The model included skin, fat, muscle, as well as the liner and prosthetic socket (**Figure 1b**).

2.2 *Mesh, Skewness and Orthogonal Quality*

After the model was imported into ANSYS CFD and the properties assigned, meshing was performed, which process involves dividing the geometry into elements and nodes. ANSYS Mesh was used to generate triangular structured uniform grid **(Figure 2a and Figure 2b)**. In ANSYS, skewness quantifies the distortion of elements within a mesh, indicating how far they deviate from ideal shapes. High skewness values indicate considerable distortion, which can affect the accuracy and stability of simulation results. Thus, minimizing skewness in the mesh helps to uphold the reliability of simulation outcomes. On the other hand, orthogonal quality measures the angles between cell faces and edges. From the mesh, the orthogonal quality was 0.77 and skewness 0.23 which is found to be within acceptable range (**Table 1**).

`

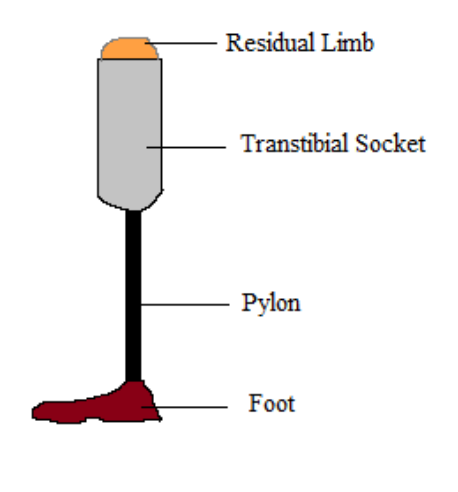


Figure 1(a): Diagram of a residual limb in a lower limb prosthesis

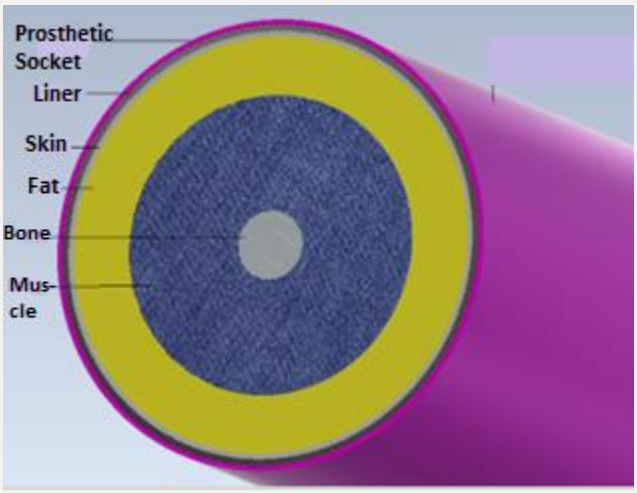


Figure 1(b): Representation of the 3D model used in the current study

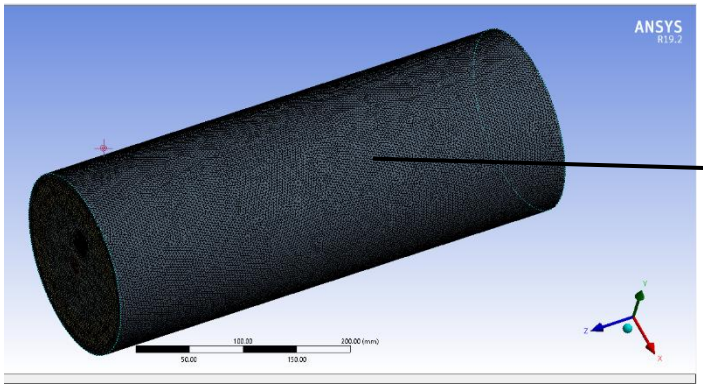


Figure 2(a): View of the structured mesh

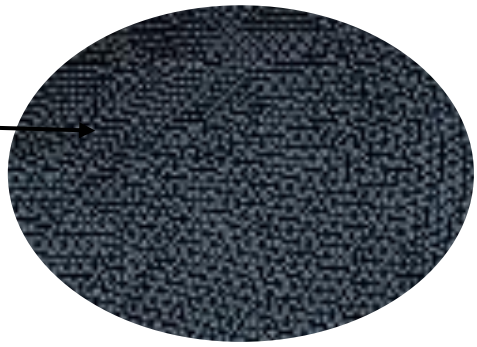


Figure2(b): A cut-out and zoomed in portion of the mesh

Table 1: Mesh quality report

Mesh Quality	Value	Acceptable Range (Source: Fatchurrohman and Chia, 2017)
Orthogonal Quality	0.77	0.15 – 1.00
Skewness	0.23	0.00 – 0.94

2.3 Governing Equations

The Pennes bioheat equation was used as the bio heat model. The rate of thermal energy accumulation of the tissue, based on the passive system (that is a body not undergoing exercise or activity or is in basal state), is:

$$\rho_t c_t \frac{\partial T_t}{\partial t} = \nabla \cdot (k_t \nabla T_t) + \rho_b c_b \omega_b (T_b - T_t) + q_{m,\text{bas}} \quad (1)$$

When the body is no longer at rest (basal state) and is involved in an activity such as walking or running, the body heats up the working muscles in proportion to the amount of work it performs. Hence, Eq. 1 is now modified and the equation for activity becomes:

`

$$\rho_t c_t \frac{\partial T_t}{\partial t} = \nabla \cdot (k_t \nabla T_t) + \rho_b c_b \omega_b (T_b - T_t) + q_{m,\text{bas}} + q_{m,\text{act}} \quad (2)$$

For the boundary conditions, the outer surface of the prosthesis was subjected to natural convection and ambient temperature conditions, whereas the proximal end was subjected to an adiabatic boundary condition. Hence, heat transfer coefficient, h = 4 W/(m^2 K) while the ambient temperature, T = 30°C = 303 K.

The predefined material and thermal properties of the bone, muscle, skin and fat included in the simulation, excluded the need for specific boundary conditions at each interface. Moreover, the 'coupled' condition which is applied in the ANSYS Fluent boundary condition section enables the heat transfer modelling, to ensure a more accurate representation of thermal conduction across the boundaries.

2.4 Data Collection

The governing equations and boundary conditions listed above were numerically solved using a three-dimensional computational fluid dynamic code (ANSYS CFD) which uses the finite volume method. The steps in this process are outlined in the flowchart in **Figure 3**.

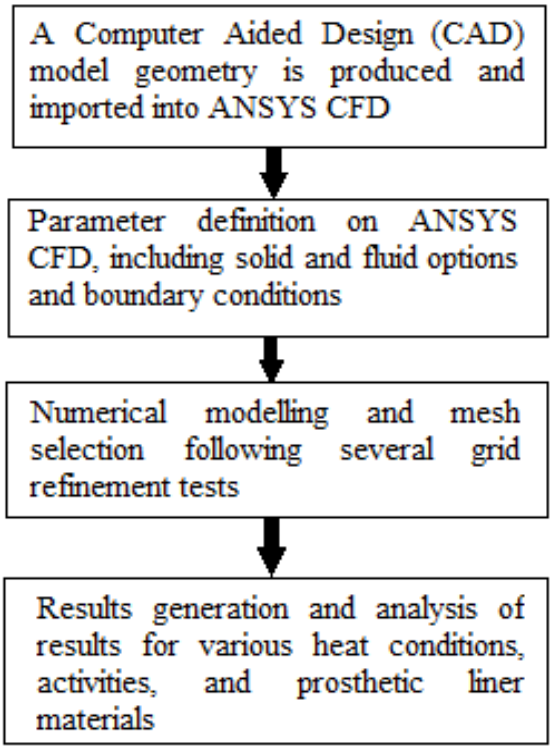


Figure 3: Steps in the process of obtaining the data from the skin-prosthesis simulation

The data obtained consist of 3600 observations points. The data obtained from the skin-prosthesis simulation were classified as time series data because they were continuous in values and discrete in time. **Figure 4** depicts a general overview of the data obtained from one set of results. The data depicted in the figure were obtained at an ambient temperature of 30°C while the user performs an activity (not resting or basal condition) for the duration of one hour while wearing the prosthesis. From the figure, it is evident that the data are initially transient and then becomes stationary after the 2000 mark. **Figure 5** shows the logarithm of the data obtained with respect to time. The logarithm was computed to stabilize the scale within the data, and make the model more reliable.

`

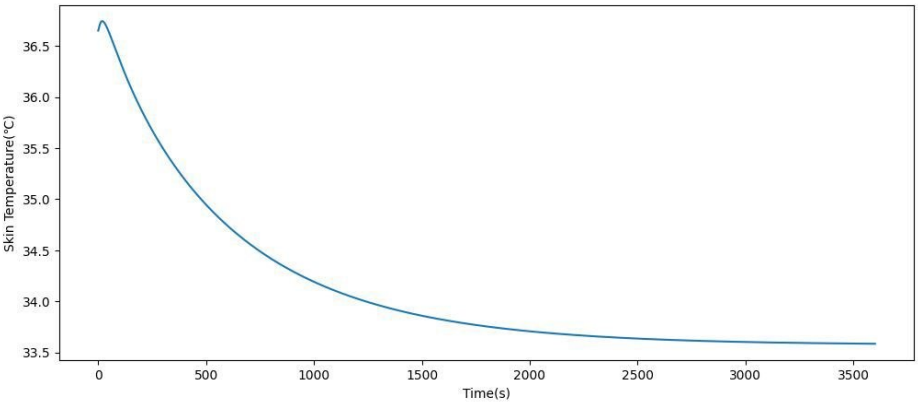


Figure 4: Recorded Skin Temperature over Time at 30°C

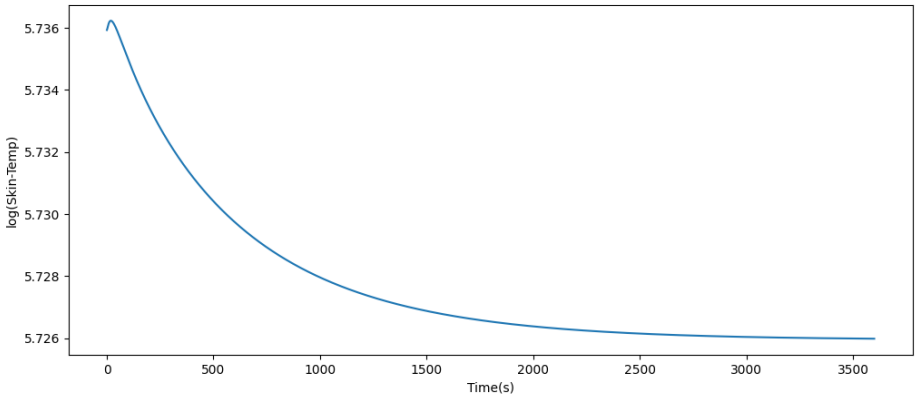


Figure 5: Log-Transformed Skin Temperature Recorded over Time at 30°C

2.5 Data Preprocessing and Forecasting using ARIMA

ARIMA model is one of the most prominent models for forecasting time-series data. The ARIMA model was used to predict and forecast values within this section. The 3600-point series was divided into training and testing subsets using an 80:20 split. The ARIMA model was fitted on the training subset (first 3000 observations), and out-of-sample forecasts were generated for the remaining 600 observations. Model performance was then evaluated by comparing the forecasts with the unseen test observations.

ARIMA allows for the forecast of long-term heat dissipation profiles for different liner materials. By comparing the predicted thermal outcomes, engineers can rank materials according to their thermal performance a priori. Clinicians and engineers can utilize this method to select or design prosthetic liners that minimize heat build-up, that leads to discomfort.

In this study, ARIMA was utilised to enhance the design of liners to ensure thermal comfort of prosthetic users. The use of the 1-hour time frame (3600 seconds) is justified because it covers the typical progression from rest to activity, allowing the temperature of the residual limb in a lower limb prosthesis to reach, or approach, a state of thermal equilibrium. It aligns with typical daily activities and covers the phase where skin temperature rises and stabilizes, often resulting in significant sweat buildup. A 1-hour simulation provides enough time for thermal insulation materials to capture relevant peak temperature levels. Experimental studies show that mean limb temperature changes within 30 minutes to 1 hour range (Edwards *et al*., 2025; Kumari and Jamal, 2023; Williams *et al*., 2019).

`

The Augmented Dickey Fuller test was conducted to determine whether the logarithm columns of the time series data obtained were stationary. The p-value obtained was less than 0.05. Thus, the result confirms that the time series test is stationary after the first difference. If the series is not stationary, it is converted into a stationary series by differencing.

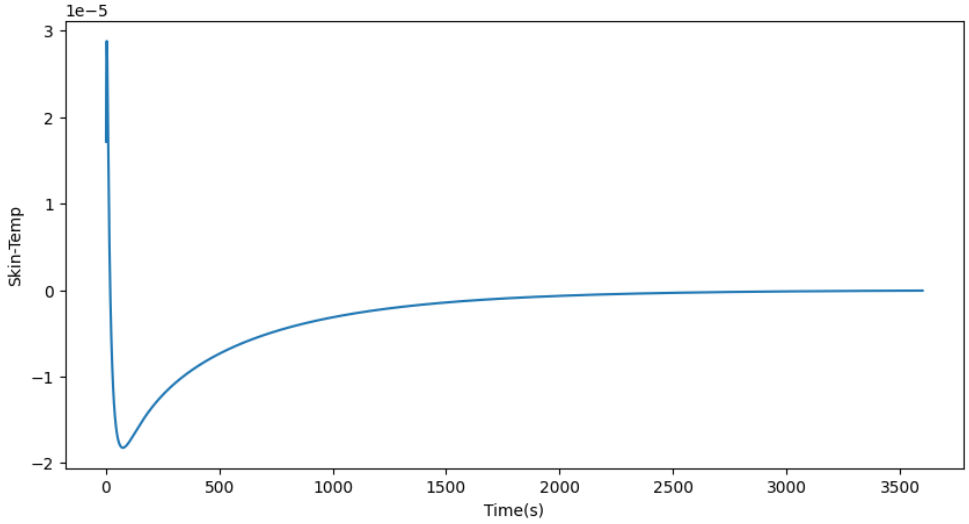


Figure 6: First difference of Recorded Skin Temperature over Time at 30 °C

After the first difference, the series becomes stationary as shown in **Figure 6**. The initial transient part fluctuates, and the rest of the data remain stationary.

The dataset was divided into training and testing subsets using an 80% – 20% split, with the training subset containing the first 3,000 observations and the testing subset comprising the subsequent 600 observations (representing future values). The training set was used to fit the ARIMA model, whereas the test set provided unseen data for evaluating and comparing the model's forecasts against actual observations. The ARIMA model works by combining three hyperparameters, p, d and q. "p" is the autoregressive part and it specifies the number of previous data points to use in the next prediction of the time series, "d" is the differencing hyperparameter and it specifies the number of times the data should be differenced, while q is the order of the moving average which specifies how many past shock errors should be used to model the next value. The governing equation for the ARIMA model is stated in Eqn. 5:

Autoregressive (AR) polynomial: $\phi_{\{p\}(B)} = 1 - \phi_{\{1\}B} - \phi_{\{2\}B}^{\{2\}} - \ldots\ldots\ldots - \phi_{\{p\}B}^{\{p\}}$ (3)

Moving Average (MA) polynomial: $\theta_{\{p\}(B)} = 1 + \theta_{\{1\}} \cdot B + \theta_{\{2\}} \cdot B^{\{2\}} + \ldots\ldots\ldots + \theta_{\{q\}} \cdot B^{\{q\}}$ (4)

Governing equation for the ARIMA model: $\phi(B)(1-B)^{\{d\}} \cdot Y_{\{t\}} = \theta_{\{q\}(B)\epsilon_{\{t\}}}$ (5)

where:

$Y_{\{t\}}$: observed time series

B: backshift operator, such that $BY_{\{t\}} = Y_{\{t-1\}}$

$\varepsilon_{\{t\}}$: white noise (error term)

d: degree of differencing

Several ARIMA configurations were fitted, and the Bayesian Information Criterion (BIC) was computed for each to identify the best performing model for the data. The BIC formula is stated in Eqn. 6. The left side indicates how well the model performs with the test data, and the right side indicates the complexity of the model (how much it depends on the inputs).

`

$$BIC = -2In(\hat{L}) + kIn(n) \quad (6)$$

The various hyperparameters tested and their BIC values is presented in **Table 2**.

Table 2: Bayesian Information criterion (BIC) for different ARIMA model configurations

ARIMA	BIC
(1, 0, 0)	-61206.1291
(2, 1, 1)	-62287.9917
(4, 1, 0)	-61278.2575
(6, 1, 1)	-62766.5196
(8, 1, 1)	-66698.1275
(9, 1, 1)	-61495.8357
(10, 1, 1)	-63343.6841

Several ARIMA configurations were compared using the Bayesian Information Criterion (BIC). BIC balances model fit and model complexity, and the model with the lowest BIC among the candidate models was selected as the preferred specification.

Based on the model selection criteria, the ARIMA (8,1,1) model was identified as the most suitable for the time-series data Consequently, further parameter tuning was deemed unnecessary for this study. The model was fitted to the training dataset, and its performance was assessed by comparing the fitted values (green curve in Figure 8) with the observed values (blue curve in **Figure 7**). Forecasts were then generated for the test period, and the predicted values are illustrated by the orange curve shown in **Figure 7**.

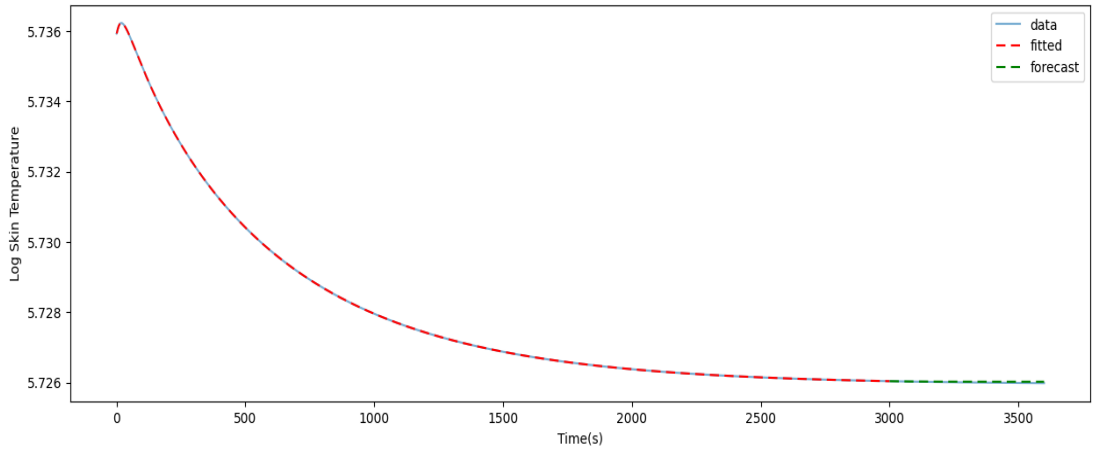


Figure 7: Graphical representation of the ARIMA model train (fitted) and test (forecast) predictions alongside the original data values

The forecasting performance of the ARIMA (8,1,1) model was assessed using the Root Mean Square Error (RMSE) and the Mean Absolute Percentage Error (MAPE). For the test period, the RMSE was 0.00736, indicating the typical magnitude of the forecast error in
the original measurement units, whereas the MAPE was 0.0020%, reflecting a very low average percentage deviation between the predicted and observed values.

3.0 RESULTS AND DISCUSSION

The actual and the predicted values of the initial 15 observations in the test set are shown in **Table 3**. Also, a chart depicting a close comparison of the first 15 observations is shown in **Figure 8**. The graphs are in good correlation with a deviation error of 3.11×10^{-7}. The chart shows an

`

overlap of both the actual and the predicted values highlighting the reliability of the model in predicting values in this range.

Table 3: Comparison of the actual and predicted values of the ARIMA (8,1,1) model for the first 15 observations of the test period

Time	Actual Values	Predicted Values	Errors/Deviations
3001	33.6023960	33.6023960	0
3002	33.6023520	33.6023520	0
3003	33.6023080	33.6023080	0
3004	33.6022640	33.6022650	0.000001
3005	33.6022200	33.6022220	0.000022
3006	33.6021760	33.6021800	0.000004
3007	33.6021320	33.6021370	0.000005
3008	33.6020880	33.6020960	0.000008
3009	33.6020440	33.6020540	0.000010
3010	33.6020010	33.6020130	0.000012
3011	33.6019570	33.6019730	0.000016
3012	33.6019130	33.6019320	0.000019
3013	33.6018700	33.6018930	0.000023
3014	33.6018270	33.6018530	0.000026
3015	33.6017830	33.6018140	0.000031

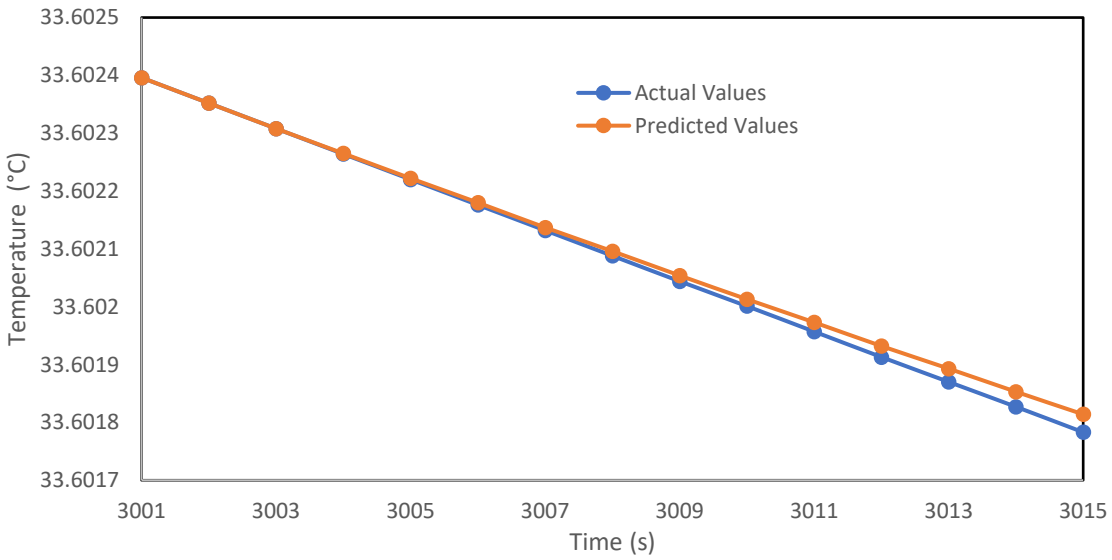


Figure 8: Actual vs. Predicted Values at 30 °C for the Initial Observations of the Test Period.

Table 4 contains the actual values and the predicted values of 15 observations obtained from the middle of the test set. **Figure 9** shows a chart comparing the actual and predicted values, the graphs are in good correlation with a deviation error of 1.93×10^{-4}.

Table 5 contains the actual values and the predicted values of 15 observations obtained from the last of the test set. **Figure 10** shows a graphical representation of the performance of the model in this data range. The chart shows a maximum of 0.000031 difference between the actual and predicted values emphasizing the model's reliability in predicting values within this range. Also, the graphs are in good correlation with a deviation error of 3.74×10^{-4}. The results show that, the model's performance is satisfactory.

`

Table 4: Comparison of the actual and predicted values of the ARIMA (8,1,1) model for the middle 15 observations of the test period

Time	Actual Values	Predicted Values	Errors/Deviations
3301	33.591760	33.598100	0.006340
3302	33.591732	33.598098	0.006366
3303	33.591705	33.598095	0.006390
3304	33.591677	33.598093	0.006416
3305	33.591650	33.598091	0.006441
3306	33.591622	33.598089	0.006467
3307	33.591595	33.598086	0.006491
3308	33.591567	33.598084	0.006517
3309	33.591540	33.598082	0.006542
3310	33.591513	33.598080	0.006567
3311	33.591485	33.598078	0.006593
3312	33.591458	33.598076	0.006618
3313	33.591431	33.598074	0.006643
3314	33.591404	33.598072	0.006668
3315	33.591760	33.598100	0.006340

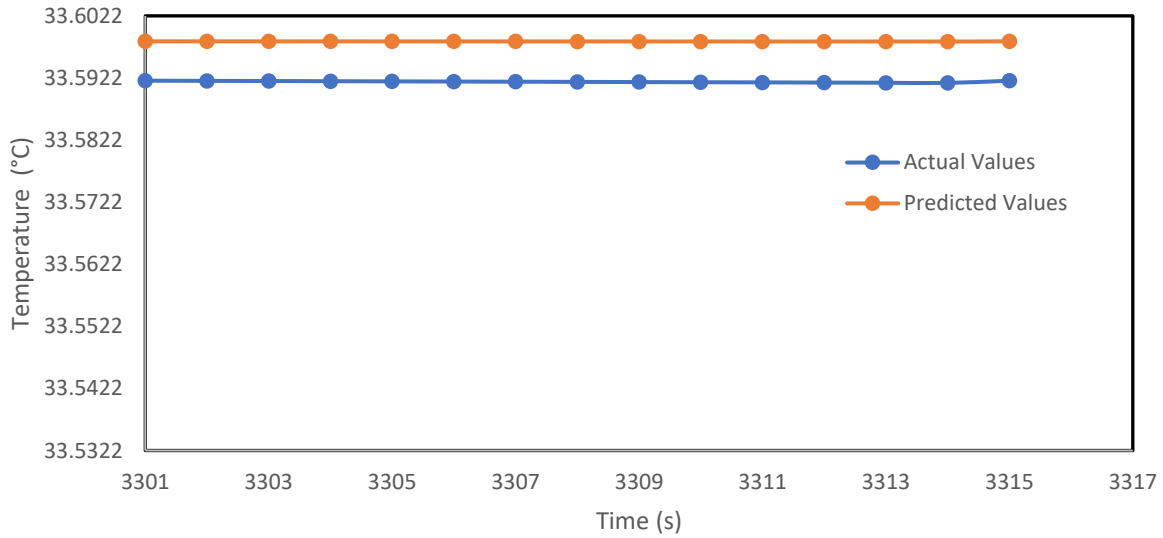


Figure 9: Actual vs. predicted values at 30 °C for the middle observations of the test period

Table 5: Comparison of the actual and predicted values of the ARIMA (8,1 ,1) model for the last 15 observations of the test period

Time	Actual Values	Predicted Values	Errors/Deviations
3586	33.585440	33.597880	0.012440
3587	33.585422	33.597880	0.012457
3588	33.585405	33.597879	0.012475
3589	33.585387	33.597879	0.012492
3590	33.585370	33.597879	0.012509
3591	33.585353	33.597879	0.012526
3592	33.585335	33.597879	0.012544
3593	33.585318	33.597879	0.012561
3594	33.585300	33.597879	0.012578
3595	33.585283	33.597878	0.012595
3596	33.585266	33.597878	0.012613
3597	33.585249	33.597878	0.012630
3598	33.585231	33.597878	0.012647
3599	33.585214	33.597878	0.012664
3600	33.585197	33.597878	0.012681

`

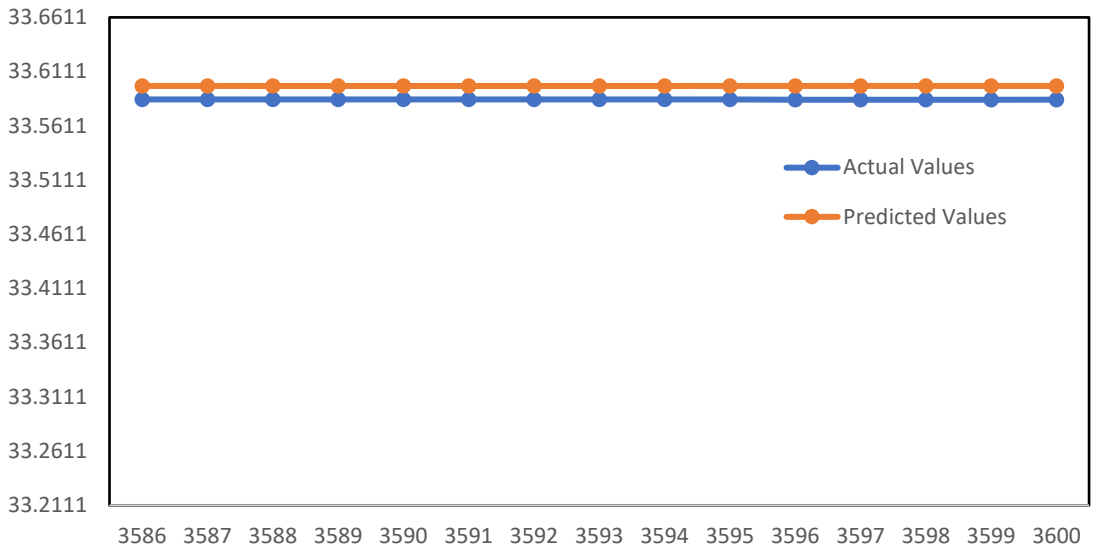


Figure 10: Actual vs. predicted Values at 30 °C for the final observations of the test period.

Model adequacy was assessed using residual diagnostics, including the residual ACF and PACF, to determine whether the fitted model successfully captured the serial dependence structure of the training series (**Figure 11** and **Figure 12**). ACF depicts the correlation between the series and its lagged values, providing insights into underlying temporal dependencies. In ARIMA modelling, the ACF is particularly useful for identifying initial test values for the moving-average (MA) order, whereas the partial autocorrelation function (PACF) is typically used to identify initial test values for the autoregressive (AR) order.

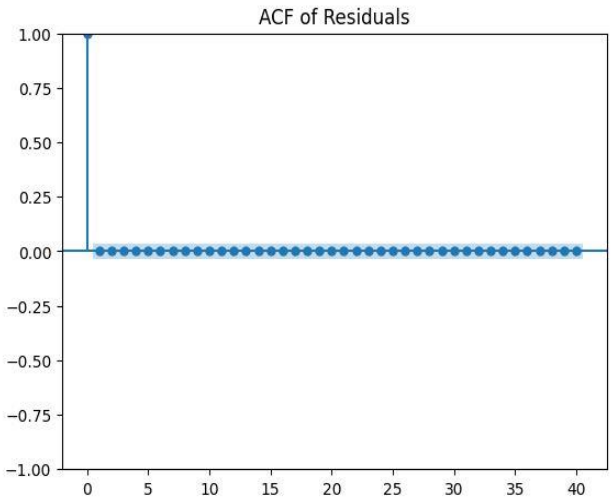


Figure 11: Autocorrelation Function (ACF) on the Residuals

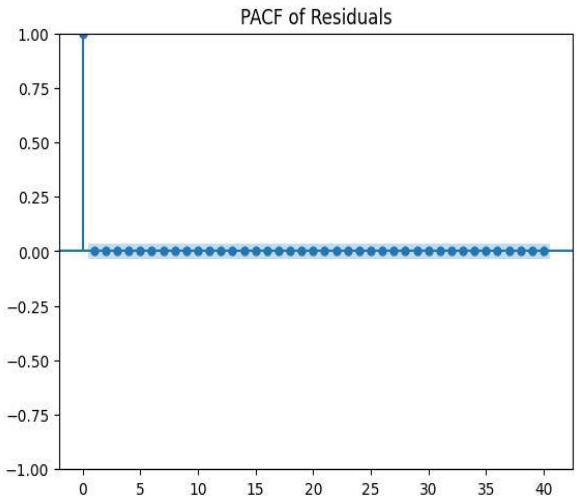


Figure 12: Partial autocorrelation function (PACF) on the residuals

4. CONCLUSION

This study developed a preliminary predictive framework for forecasting prosthetic socket temperature evolution from CFD-generated time-series data. The ARIMA model reproduced the short-horizon behaviour of the simulated temperature profile with low forecast error over the test period. However, the current study should be interpreted as a forecasting feasibility study rather than a completed liner-material optimization framework, since only limited comparative material evidence is presented.

`

ACKNOWLEDGEMENT
The authors received no specific funding for this work. Hence, the corresponding author confirms that there are no financial and personal relationships with other people or organisations that could inappropriately influence this study.

AUTHORS' CONTRIBUTIONS STATEMENT
UCU: Conceptualisation, Investigation, Data Collection, Visualisation, Software, Formal Analysis, Writing- original draft, Writing- review and editing; OTO: Review & editing of initial write-up, Research supervision; MBS: Review & editing of initial write-up; AAO: Review & editing of initial write-up; GAA: Formal analysis, Investigation, Software, Validation, Writing- original draft, Writing- review and editing, Visualisation; CPJ: Formal analysis, Investigation, Software, Validation, Writing- original draft, Writing- review and editing, Visualisation; IAF: Review & editing of initial write-up, Formal analysis, JIO: Review & editing of initial write-up, Formal analysis; AOA: Review & editing of initial write-up, Research supervision.

DATA AVAILABILITY
Datasets generated or analysed during the current study will be made available on request.

STATEMENTS AND DECLARATIONS
ETHICAL
The current study did not include any human or animal subjects. Thus, this study is not subject to an ethics review committee and does not require any informed consent.
COMPETING INTERESTS
The authors declare that they have no known competing financial or non-financial interests or personal relationships that could have appeared to influence the work reported in this paper.

REFERENCES
Abbood, S. A., Wu, Z., and Sundén, B. (2017). Thermal assessment for prostheses: State-of-the-art review. International Journal of Computational Methods and Experimental Measurements, 5(1), 1-12.

Diment, L. E., Thompson, M. S., and Bergmann, J. H. (2019). Comparing thermal discomfort with skin temperature response of lower-limb prosthesis users during exercise. Clinical Biomechanics, 69, 148-155.

Edwards, R., Murray, L., and Buis, A. (2025). The role of human thermoregulation in thermal discomfort in lower-limb prosthetics: a scoping review. Canadian Prosthetics & Orthotics Journal, 8(1).

Fatchurrohman, N., and Chia, S. T. (2017, October). Performance of hybrid nano-micro reinforced mg metal matrix composites brake calliper: simulation approach. In IOP conference series: materials science and engineering (Vol. 257, No. 1, p. 012060). IOP Publishing.

Feng, G., Zhang, L., Ai, F., Zhang, Y., and Hou, Y. (2022). An improved temporal fusion transformers model for predicting supply air temperature in high-speed railway carriages. Entropy, 24(8), 1111.

Fiedler, G., Singh, A., and McKernan, G. (2022). Does socket liner material affect clinical outcomes in lower limb prosthesis users? Insights from a randomized control trial. Prosthetics and Orthotics International, 46(2), 199-201.

Ghoseiri, K., and Safari, R. (2014). Prevalence of heat and perspiration discomfort inside prostheses: Literature review. Journal of Rehabilitation Research and Development.

`

Gnyawali, S. C., Denune, J. A., Hockman, B., Kristjánsdóttir, J. V., Ragnarsdóttir, M. S., Timsina, L. R., ... and Roy, S. (2023). Moisture mitigation using a vented liner and a vented socket system for individuals with transfemoral amputation. Scientific Reports, 13(1), 16557.

Kaur, J., Parmar, K. S., and Singh, S. (2023). Autoregressive models in environmental forecasting time series: a theoretical and application review. Environmental Science and Pollution Research, 30(8), 19617-19641.

Kumari, R., and Jamal, T. (2023). Residual limb temperature study with Pe-Lite liner in traumatic transtibial amputees.

Lee, K. H., Heo, H. S., Kim, J., Cho, J. H., Kim, K. T., Hur, J. Y., ... & Lee, Y. (2023). A pneumatically controlled prosthetic socket for transfemoral amputees. Sensors, 24(1), 133.

Mathur, N., Glesk, I., and Buis, A. (2016). Thermal time constant: Optimising the skin temperature predictive modelling in lower limb prostheses using Gaussian processes. Healthcare Technology Letters, 3(2), 98-104.

Nurhanisah, M. H., Jawaid, M., Ahmad Azmeer, R., and Paridah, M. T. (2019). The AirCirc: Design and development of a thermal management prototype device for below-knee prosthesis leg socket. Disability and Rehabilitation: Assistive Technology, 14(5), 513-520.

Paternò, L., Dhokia, V., Menciassi, A., Bilzon, J., and Seminati, E. (2020). A personalised prosthetic liner with embedded sensor technology: A case study. Biomedical Engineering Online, 19(1), 71.

Patharkar, A., Cai, F., Al-Hindawi, F., and Wu, T. (2024). Predictive modeling of biomedical temporal data in healthcare applications: review and future directions. Frontiers in physiology, 15, 1386760.

Schaffer, A. L., Dobbins, T. A., and Pearson, S. A. (2021). Interrupted time series analysis using autoregressive integrated moving average (ARIMA) models: a guide for evaluating large-scale health interventions. BMC medical research methodology, 21(1), 58.

Williams, R. J., Takashima, A., Ogata, T., and Holloway, C. (2019). A pilot study towards long-term thermal comfort research for lower-limb prosthesis wearers. Prosthetics and Orthotics International, 43(1), 47-54.

Williams, R. J. (2020). Exploring thermal discomfort amongst lower-limb prosthesis wearers (Doctoral dissertation, University College London). Retrieved from https://discovery.ucl.ac.uk/id/eprint/10095050/

`